Check for updates

Interaction with prefibrillar species and amyloid-like fibrils changes the stiffness of lipid bilayers†

Bruno C. Borro, [a] Lucia Parolini, [b] Pietro Cicuta, [b] Vito Foderà ‡*[a] and Lorenzo Di Michele ‡*[b]

Evaluating the toxicity of self-assembled protein states is a key step towards developing effective strategies against amyloidogenic pathologies such as Alzheimer's and Parkinson's diseases. Such analysis is directly connected to quantitatively probing the stability of the cellular membrane upon interaction with different protein states. Using a combination of spectroscopic techniques, morphological observations, and spectral analysis of membrane fluctuations, we identify different destabilisation routes for giant unilamellar vesicles interacting with native-like states, prefibrillar species and amyloid-like fibrils of α-lactalbumin. These effects range from substantially lowering the bending rigidity of the membranes to irreversible structural changes and complete disruption of the lipid bilayers. Our findings clearly indicate how the wide heterogeneity in structures occurring during protein aggregation can result in different destabilisation pathways, acting on different length scales and not limited to enhanced membrane permeability.

Amyloid pathologies such as Alzheimer's and Parkinson's diseases are characterised by the accumulation of protein deposits in tissues, namely amyloid fibrils, but it is still debated whether fibrils are a cause or a by-product in the disease progression.[1] Increasing evidence shows that, in the presence of either small protein oligomers or fibrils, cell lipid membranes are highly destabilised.[2,3] This results in a modification of the cell permeability and ultimately cell death.[1–3] While understanding protein aggregation is pivotal to design strategies for effective inhibition of the process, approaches to protect the cell membranes or enhance their stability could represent alternative ways to

prevent the progression of the diseases. To date, studies on membrane stability in the presence of amyloidogenic proteins have mainly focused on quantifying leakage.[4–7] Although this approach enables to determine some of the mechanisms leading to membrane disruption, it does not allow the identification of which specific features of the protein species are causing the damage, nor to what extent. In fact, the size, secondary structure and exposure of specific amino-acids are factors that could affect the toxicity of protein species, some of which could cause physical changes to the bilayers without necessarily contributing to the membrane permeability. In this context, a key role is attributed to the toxic potency of oligomeric or prefibrillar species. These species present a high structural and morphological heterogeneity in terms of size,[8] shape,[9] compactness,[10] stability,[11,12] and secondary and tertiary structure contents.[13] Often referred to as polymorphism,[14] such variability likely implicates different potential interactions with membranes, which may not be detectable by leakage experiments or by qualitative morphological investigation, but still play a crucial role in membrane destabilisation. This calls for a quantitative evaluation of the intrinsic physical properties of lipid bilayers in the presence of different proteins states prior to the actual disruption.

In this communication, we study how different protein conformational states and aggregation states alter giant uni-lamellar vesicles (GUVs) prepared from 1,2-dioleoyl-*sn-glycero*-3-phosphocholine (DOPC), with a focus on the morphology and intrinsic physical properties of the membrane, specifically its bending rigidity estimated by flickering spectroscopy.[15,16] α-Lactalbumin (ALA) is chosen as a protein model system.[17,18] We find that partially unfolded monomers and protein aggregates segregate onto the bilayers, but only the presence of aggregates can perturb the morphology and stiffness of the membrane. Among aggregates, prefibrillar species are less disruptive than mature fibrils, but both types of aggregates cause a similar "softening" of the exposed bilayers. Our data point towards a novel multifaceted scenario for protein-induced disruption of membranes, in which different destabilisation mechanisms act on different length scales.

[a] Section for Biologics, Dept. of Pharmacy, University of Copenhagen, Universitetsparken 2, 2100 Copenhagen, Denmark. E-mail: vito.fodera@sund.ku.dk

[b] Biological and Soft Systems, Cavendish Laboratory, University of Cambridge, Cambridge, CB3 0HE, UK. E-mail: ld389@cam.ac.uk

† Electronic supplementary information (ESI) available: Materials, protein sample preparation and characterisation, GUV preparation, sample preparation, confocal microscopy imaging and flickering measurements, examples of flickering videos, and analysis of flickering data. See DOI: 10.1039/c7cp05339h

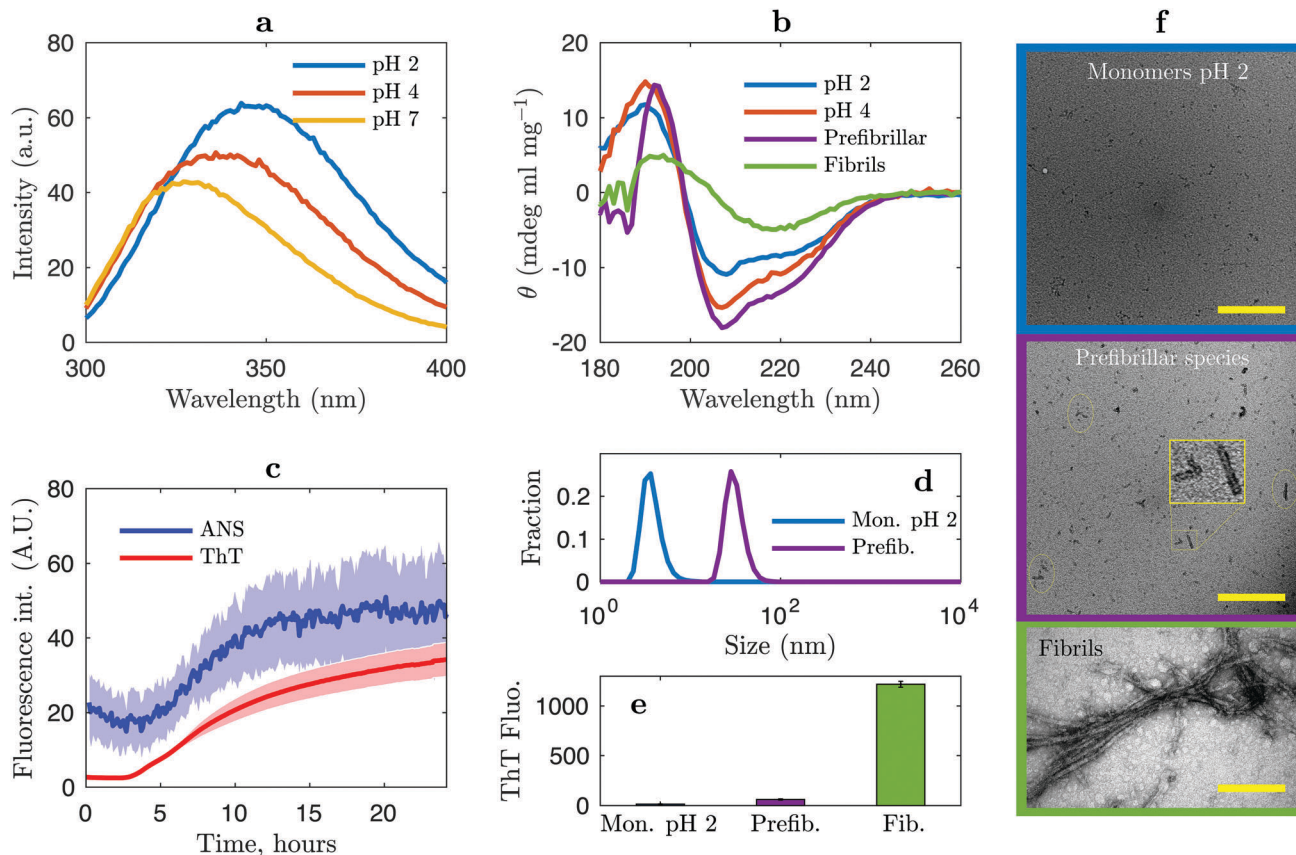‡ These authors contributed equally.

Fig. 1 Preparation, isolation, and characterisation of the ALA states. (a) Tryptophan fluorescence band of native-like samples; (b) synchrotron radiation circular dichroism (SRCD) spectra of native-like samples, prefibrillar species and fibrils. Spectra are normalised by the sample concentration; (c) thermally induced ALA aggregation kinetics at pH 2 and at 60 °C probed by ANS and ThT. The ThT curve was divided by 80 units to fit the fluorescence scale; (d) size distribution by number of species of monomers prepared at pH 2 and prefibrillar species as measured by dynamic light scattering (DLS); (e) 20 μM ThT fluorescence intensity in the presence of monomers, prefibrillar species and fibrils; (f) representative transmission electron microscopy (TEM) images of the ALA samples in the monomeric state at pH 2 (top), prefibrillar species (middle, isolated after 10 h of treatment at 60 °C and pH 2) and amyloid-like fibrils (bottom, after 24 hours of thermal treatment at 60 °C and after the removal of residual soluble species by centrifugation at pH 2). The scale bars are 500 nm (top and middle) and 200 nm (bottom).

Different conformational states are generated by dissolving ALA at pH 7, pH 4 and pH 2 (see ESI†). To evaluate the degree of folding for these native-like states, we monitor the tryptophan (Trp) fluorescence, detecting a red shift of the Trp emission peak and a simultaneous increase of the fluorescence intensity when going from pH 7 to pH 2 (Fig. 1a). This stems from an increased exposure of the ALA hydrophobic core, which translates into an increasingly less compact and more open structure.[19] The peculiar signature in the synchrotron radiation circular dichroism (SRCD) spectra (Fig. 1b), namely the presence of minima at 208 and 222 nm, indicates that the protein retains a α-helical structure at both pH 4 and pH 2. The combined evidence of Trp fluorescence and SRCD experiments indicates that two different types of the molten globule state with different compactness are likely formed at pH 4 and 2.[19]

To produce aggregates, the ALA self-assembly was induced at pH 2 by incubating the sample at 60 °C (see ESI†). Under these conditions, ALA readily aggregates within 24 hours. The amyloid-marker thioflavin T (ThT) shows indeed a growth of amyloid-like aggregates after a lag time of approximately

3 hours (Fig. 1c). In parallel we monitor the accessibility of hydrophobic binding sites during the aggregation kinetics via 8-anilinonaphthalene-1-sulfonic acid (ANS) fluorescence.[20] Data suggest a gradual increase in the exposure of the protein interior while the aggregation proceeds (Fig. 1c). We produce prefibrillar species via centrifugation of the samples after 10 hours of incubation, when the fibrillation process is still incomplete (see ESI†). This procedure ensures the separation of a mixture of prefibrillar/oligomeric species (not converted into fibrils) from the already formed fibrils. From now on we refer to this mixture as "prefibrillar species". DLS measurements reveal indeed the presence of high molecular weight species with an effective diameter of 80 nm in this mixture (Fig. 1d, size distribution by number of species). The disappearance of the peak related to the monomer in Fig. 1d confirms that the concentration of the monomer is likely to be negligible in the prefibrillar species sample. SRCD spectra highlight an enhanced α-helix content of the so-prepared species as compared to the pure monomeric samples at pH 2 and 4 (Fig. 1b). We also perform a ThT test on the prefibrillar species, showing a level of

fluorescence comparable to the pure monomeric species (Fig. 1e). This indirectly confirms the negligible presence of β-sheet structure in such a sample. The presence of prefibrillar species in the size range of 100 nm is also detectable by transmission electron microscopy (TEM) (Fig. 1f, middle, magnification in the yellow box) when compared to the pure monomeric sample (Fig. 1f, top). Fibrils are isolated from the incubated samples after 24 hours of incubation (see ESI†). Aggregates present elongated μm-long morphologies (Fig. 1f, bottom) rich in β-sheet structure (minimum at 220 nm in the SRCD spectra, Fig. 1b, and high ThT fluorescence, Fig. 1e), confirming the presence of amyloid-like fibrils. Once different protein species are isolated, we addressed the following questions: can we quantitatively relate the structural and physico-chemical features of these species to their effect on the morphology and flexibility of the membrane? And, ultimately, can we identify different mechanisms affecting the bilayer stability?

Confocal microscopy images in Fig. 2a reveal how in samples prepared at pH 7 fluorescently labelled protein (red) does not interact with the GUVs (cyan): the protein remains uniformly suspended in the solution. In samples prepared at pH 2 and pH 4, instead, the proteins show a clear affinity for the bilayer, demonstrated by the enhanced red-fluorescence on the contour of the vesicles (Fig. 2b and c). This allows us to draw a first conclusion: slightly open structures exposing hydrophobic residues (pH 2 and 4) are more likely to interact with GUVs compared to more compact structures (pH 7). Such interaction, however, does not seem to affect the vesicle morphology, and

deformation/defects are barely detectable within the microscope resolution. At these acidic pH values, both ALA and DOPC liposomes have a net positive charge, so electrostatics cannot be responsible for the protein-membrane affinity.[21,22]

Similarly, we investigate the effects of prefibrillar species and amyloid-like fibrils. Before exposing them to the GUVs, mature fibrils were sonicated to break up large aggregates (see the ESI† for details). Both fibrils and prefibrillar species have a strong tendency to partition onto the membranes, and both cause significant morphological changes to the vesicles. The nature of such changes is however qualitatively and quantita-tively distinct. The prefibrillar species tend to produce more localised defects, visible as small fluorescent lumps in Fig. 2d, without significantly altering the spherical shape of the liposomes. Instead, Fig. 2e shows how amyloid-like fibrils cause severe deformations: some (although not all) vesicles look crumpled, with large areas where the bilayer is clearly disrupted. The morpho-logical analysis would lead one to conclude that the physical damage produced by amyloid-like fibrils on the bilayers is much more pronounced compared to the one caused by prefibrillar species. While this is true in terms of macroscopic effects (related to the potency in disrupting the membrane), it is worth investi-gating the consequences that protein aggregates have on the physical properties of the bilayer, not immediately evident from qualitative observations.

The bending modulus κ is an intrinsic property of the lipid bilayers, often adopted as an indicator for the occurrence of
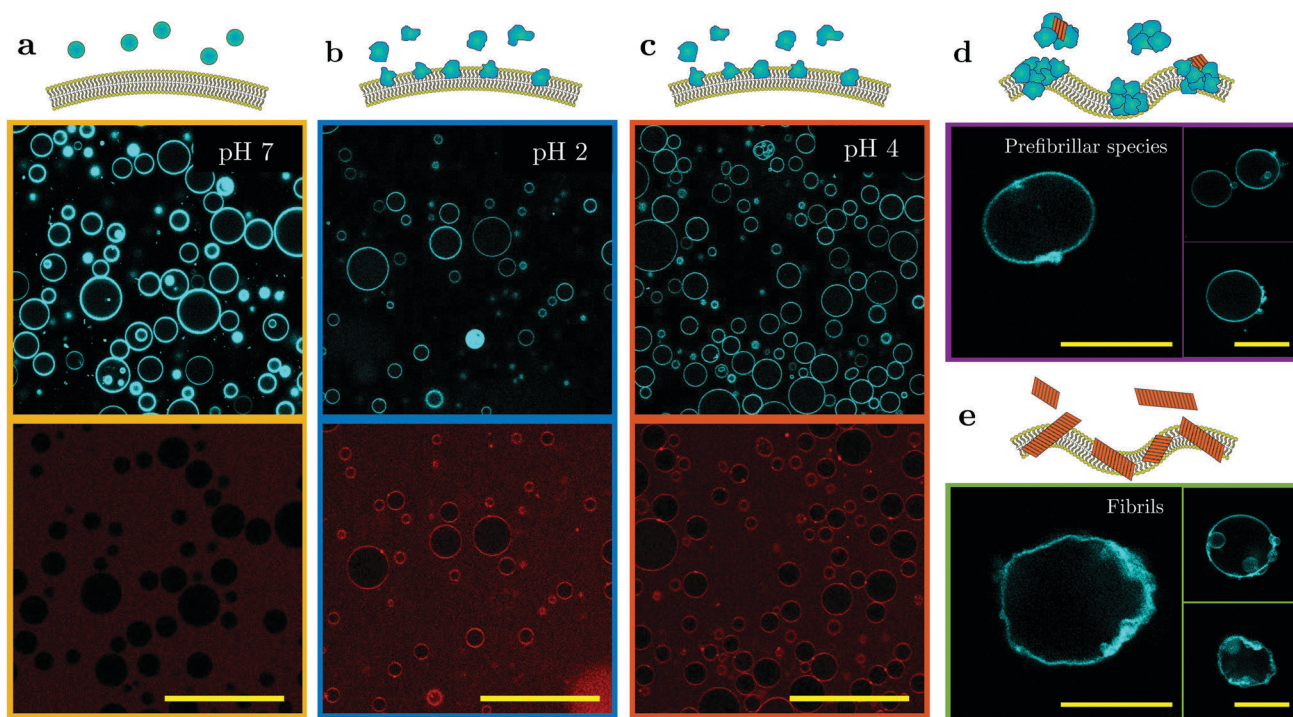

Fig. 2 Exposure of hydrophobic groups and aggregation state influence protein-bilayer interaction and membrane disruption. Native-like ALA at (a) pH 7, (b) pH 2 and (c) pH 4. In (a)–(c) ALA is labelled with Atto 647 N and shown in red (bottom), GUVs are labelled with 0.8% molar fraction of Oregon Green 488 1,2-dihexadecanoyl-*sn-glycero*-3-phosphoethanolamine (DHPE) and shown in cyan (top). Scale bars are 100 μm. (d and e) GUVs upon interaction with (d) ALA prefibrillar species and (e) ALA amyloid-like fibrils. Vesicles are labelled with 0.8% molar fraction of Texas Red DHPE and shown in cyan. Scale bars are 20 μm.

structural changes induced by inclusions. We estimate κ via flickering spectroscopy. High frame-rate confocal videos of the vesicles' equator are recorded, and the time-dependent contour is reconstructed my means of a tailor-made software.[16] Fourier analysis enables the evaluation of the mean-squared amplitude of the equatorial fluctuation modes, which are then fitted to a model to extract κ (see ESI†).[24] Note that flickering requires "clean" equatorial contours, thus only vesicles not showing major structural defects within the microscope resolution could be analyzed (see the ESI† for examples of videos).

Fig. 3 summarises the distribution of bending moduli as recorded in the presence of the different protein species and for "bare" DOPC GUVs at pH 2. Although the exposed hydrophobic residues in the samples at pH 4 and pH 2 (Fig. 1a) cause the protein molecules to partition onto the membranes (Fig. 2a–c, bottom), we find the mean κ values of $23.6 \pm 1.9 k_{B}T$ and $21.5 \pm 1.3 k_{B}T$ respectively, only a small reduction as compared to the value recorded for bare GUVs ($27.2 \pm 1.1 k_{B}T$). We can thus conclude that the incorporation of partially unfolded monomeric species does not significantly affect the morphology nor the intrinsic mechanical features of the bilayers. Prefibrillar species and fibrils have a much larger effect on κ, reducing it to $11.3 \pm 0.9 k_{B}T$ and $14.5 \pm 1.1 k_{B}T$, respectively. This means that, unlike the native-like states, prefibrillar species and fibrils cause a "softening" of the bilayers upon insertion. In addition to this, and within the statistical ensemble analyzed, we observe a slightly more pronounced rigidity decrease in the samples exposed to prefibrillar species compared to fibrils (see distributions in Fig. 3). The fact that prefibrillar species can
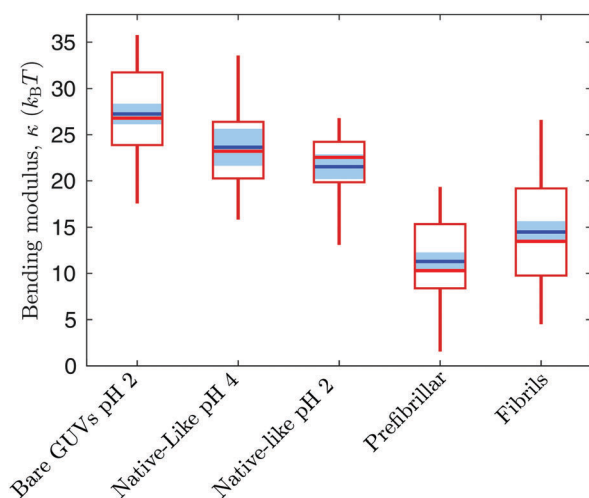

Fig. 3 ALA aggregates cause bilayer softening. Boxplots showing the distribution of the bending modulus values for each system. The red segment dividing the box indicates the median of the distribution, where the boxes enclose the data between the 25th and the 75th percentiles. The bars indicate the maximum and minimum of each distribution. The mean values and standard errors are presented as solid blue lines and blue rectangles, respectively. Note that the bending module value of $27.2 \pm 1.1 k_{B}T$, recorded for bare GUVs at pH 2, is compatible with the outcome of flickering measurements on DOPC membranes at neutral pH,[23] indicating that the pH change alone does not cause measurable mechanical changes.

affect membrane deformability to the same (or to a greater) extent as the fibrils comes as a surprise, in view of the clear difference in the magnitude of induced morphological disruption (Fig. 2d and e). While the latter can be detected by morphological analysis and leakage experiments, the subtle change in the intrinsic deformability of the lipid bilayer would have been hidden without a quantitative mechanical characterisation.

The possibility to form prefibrillar species or oligomers mainly retaining the native-like structural features has been observed for several systems.[25–28] In different protein systems, the α to β transition of oligomers is often observed.[14] This means that as aggregation proceeds, prefibrillar species undergo a structural rearrangement into species stabilised by a specific structure, an increase in dimensions and compactness.[12,14] Depending on these variables, prefibrillar species present different cytotoxic effects.[14] Our data show that α-helix rich prefibrillar species can cause substantial physical changes to the membrane, without showing a large-scale disruption. The ability of such structures to affect the membrane stiffness to a much greater extent compared to the native-like samples can mainly be due to the presence of high molecular weight species (Fig. 1f, middle) and, likely, the overall enhanced α-helix content. The latter is indeed indicated as a crucial feature for membrane insertion. As an example, upon interaction with lipid bilayers, α-synuclein can adopt α-helical conformations and modify the physico-chemical properties of the membrane, eventually leading to disruption.[29] However, α-synuclein produces an increase in bending rigidity, rather than softening the membranes. The opposite effects of α-synuclein and ALA on lipid bilayers may appear inconsistent. Likewise, our finding that ALA inclusions cause membrane softening rather than stiffening may itself seem counterintuitive. Indeed, in the simplest picture where they are considered as rigid inclusions, the sole effect of membrane binding proteins should be to increase κ.[30] There is, however, increasing experimental evidence of functional proteins causing membrane softening; remarkable examples include antibiotic peptides[31] and the HIV-fusion peptides,[32] believed to facilitate viral infection. The mechanism through which these proteins soften the membrane could be mainly related to a local structural rearrangement of lipids around the inclusion, causing a decrease in membrane thickness.[30] The details of lipid rearrangement depend on the protein structure and the hydrophobicity and hydrophilicity of the amino acids, explaining the heterogeneous behaviours observed across different species.

Considering the overall ALA aggregation process, the softening induced by prefibrillar species may certainly facilitate the membrane disruption once β-sheet-rich structures are formed (i.e., fibrils). Moreover, both fibrils and prefibrillar species can also occur simultaneously during an aggregation process. Such a scenario forces one to consider the protein-induced membrane disruption as a multi-step process. The physico-chemical characterisation of the protein species and the combined assessment of the morphological and mechanical features of the membranes exposed to such samples allowed us to identify different routes via which self-assembled proteins can influence a lipid bilayer. This is particularly significant for the analysis of

medically-relevant systems in which a range of structurally different oligomers has been identified.[14] One could easily foresee the application of our approach to distinguish the different toxic potencies of the so-far-isolated multiple oligomeric species of Aβ peptide[33] and α-synuclein,[33,34] involved in Alzheimer's and Parkinson's diseases, respectively. Such analysis would create a univocal link between oligomer structures and physico-chemical properties, and their role in the onset and progress of pathologies.

Conflicts of interest

There are no conflicts of interest to declare.

Acknowledgements

References

1 S. A. Kotler, P. Walsh, J. R. Brender and A. Ramamoorthy, *Chem. Soc. Rev.*, 2014, **43**, 6692–6700.

2 M. Bucciantini, S. Rigacci and M. Stefani, *J. Phys. Chem. Lett.*, 2014, **5**, 517–527.

3 S. Campioni, B. Mannini, M. Zampagni, A. Pensalfini, C. Parrini, E. Evangelisti, A. Relini, M. Stefani, C. M. Dobson, C. Cecchi and F. Chiti, *Nat. Chem. Biol.*, 2010, **6**, 140–147.

4 A. Kastorna, V. Trusova, G. Gorbenko and P. Kinnunen, *Chem. Phys. Lipids*, 2012, **165**, 331–337.

5 W. Qiang, W.-M. Yau and J. Schulte, *Biochim. Biophys. Acta, Biomembr.*, 2015, **1848**, 266–276.

6 J. R. Brender, E. L. Lee, M. A. Cavitt, A. Gafni, D. G. Steel and A. Ramamoorthy, *J. Am. Chem. Soc.*, 2008, **130**, 6424–6429.

7 M. F. M. Sciacca, S. A. Kotler, J. R. Brender, J. Chen, D.-K. Lee and A. Ramamoorthy, *Biophys. J.*, 2012, **103**, 702–710.

8 I. A. Mastrangelo, M. Ahmed, T. Sato, W. Liu, C. Wang, P. Hough and S. O. Smith, *J. Mol. Biol.*, 2006, **358**, 106–119.

9 D. L. Pountney, N. H. Voelcker and W. P. Gai, *Neurotoxic. Res.*, 2005, **7**, 59–67.

10 J. Kaylor, N. Bodner, S. Edridge, G. Yamin, D.-P. Hong and A. L. Fink, *J. Mol. Biol.*, 2005, **353**, 357–372.

11 P. O. Souillac, V. N. Uversky and A. L. Fink, *Biochemistry*, 2003, **42**, 8094–8104.

12 M. Calamai, C. Canale, A. Relini, M. Stefani, F. Chiti and C. M. Dobson, *J. Mol. Biol.*, 2005, **346**, 603–616.

13 N. L. Fawzi, J. Ying, R. Ghirlando, D. A. Torchia and G. M. Clore, *Nature*, 2011, **480**, 268–272.

14 F. Bemporad and F. Chiti, *Chem. Biol.*, 2012, **19**, 315–327.

15 Y.-Z. Yoon, H. Hong, A. Brown, D. C. Kim, D. J. Kang, V. L. Lew and P. Cicuta, *Biophys. J.*, 2009, **97**, 1606–1615.

16 S. F. Shimobayashi, B. M. Mognetti, L. Parolini, D. Orsi, P. Cicuta and L. Di Michele, *Phys. Chem. Chem. Phys.*, 2015, **17**, 15615–15628.

17 E. A. Permyakov and L. J. Berliner, *FEBS Lett.*, 2000, **473**, 269–274.

18 J. Goers, S. E. Permyakov, E. A. Permyakov, V. N. Uversky and A. L. Fink, *Biochemistry*, 2002, **41**, 12546–12551.

19 A. Chaudhuri, S. Haldar and A. Chattopadhyay, *Biochem. Biophys. Res. Commun.*, 2010, **394**, 1082–1086.

20 V. Vetri, M. Leone, L. A. Morozova-Roche, B. Vestergaard and V. Foderà, *PLoS One*, 2013, **8**, e68912.

21 M. J. Kronman, R. Andreotti and R. Vitols, *Biochemistry*, 1964, **3**, 1152–1160.

22 F. Quemeneur, M. Rinaudo and B. Pépin-Donat, *Biomacromolecules*, 2008, **9**, 396–402.

23 S. A. Rautu, D. Orsi, L. Di Michele, G. Rowlands, P. Cicuta and M. S. Turner, *Soft Matter*, 2017, **13**, 3480–3483.

24 J. Pécréaux, H. G. Döbereiner, J. Prost, J. F. Joanny and P. Bassereau, *Eur. Phys. J. E: Soft Matter Biol. Phys.*, 2004, **13**, 277–290.

25 L. Banci, I. Bertini, N. D'Amelio, E. Gaggelli, E. Libralesso, I. Matecko, P. Turano and J. S. Valentine, *J. Biol. Chem.*, 2005, **280**, 35815–35821.

26 A. Olofsson, J. H. Ippel, S. S. Wijmenga, E. Lundgren and A. Öhman, *J. Biol. Chem.*, 2004, **279**, 5699–5707.

27 K. Pagano, F. Bemporad, F. Fogolari, G. Esposito, P. Viglino, F. Chiti and A. Corazza, *J. Biol. Chem.*, 2010, **285**, 14689–14700.

28 M. Bouchard, J. Zurdo, E. J. Nettleton, C. M. Dobson and C. V. Robinson, *Protein Sci.*, 2000, **9**, 1960–1967.

29 A. van Maarschalkerweerd, V. Vetri, A. E. Langkilde, V. Foderà and B. Vestergaard, *Biomacromolecules*, 2014, **15**, 3643–3654.

30 H. Agrawal, M. Zelisko, L. Liu and P. Sharma, *Sci. Rep.*, 2016, **6**, 25412EP.

31 J. Pan, D. P. Tieleman, J. F. Nagle, N. Kučerka and S. Tristram-Nagle, *Biochim. Biophys. Acta, Biomembr.*, 2009, **1788**, 1387–1397.

32 S. Tristram-Nagle and J. F. Nagle, *Biophys. J.*, 2007, **93**, 2048–2055.

33 I. F. Tsigelny, L. Crews, P. Desplats, G. M. Shaked, Y. Sharikov, H. Mizuno, B. Spencer, E. Rockenstein, M. Trejo, O. Platoshyn, J. X. J. Yuan and E. Masliah, *PLoS One*, 2008, **3**, e3135.

34 M. Andreasen, N. Lorenzen and D. Otzen, *Biochim. Biophys. Acta, Biomembr.*, 2015, **1848**, 1897–1907.